DIVISION S-5—PEDOLOGY

Pedogenic Silica Accumulation in Chronosequence Soils, Southern California

Katherine J. Kendrick* and Robert C. Graham

ABSTRACT

Chronosequential analysis of soil properties has proven to be a valuable approach for estimating ages of geomorphic surfaces where no independent age control exists. In this study we examined pedogenic silica as an indicator of relative ages of soils and geomorphic surfaces, and assessed potential sources of the silica. Pedogenic opaline silica was quantified by tiron (4,5-dihydroxy-1,3-benzene-disulfonic acid [disodium salt], $C_6H_4Na_2O_8S_2$) extraction for pedons in two different chronosequences in southern California, one in the San Timoteo Badlands and one in Cajon Pass. The soils of both of these chronosequences are developed in arkosic sediments and span 11.5 to 500 ka. The amount of pedogenic silica increases with increasing duration of pedogenesis, and the depth of the maximum silica accumulation generally coincides with the maximum expression of the argillic horizon. Pedogenic silica has accumulated in all of the soils, ranging from 1.2% tiron-extractable Si (Si_{tn}) in the youngest soil to 4.6% in the oldest. Primary Si decreases with increasing duration of weathering, particularly in the upper horizons, where weathering conditions are most intense. The loss of Si coincides with the loss of Na and K, implicating the weathering of feldspars as the likely source of Si loss. The quantity of Si lost in the upper horizons is adequate to account for the pedogenic silica accumulation in the subsoil. Pedogenic silica was equally effective as pedogenic Fe oxides as an indicator of relative soil age in these soils.

Soil properties that change with duration and intensity of weathering have been used in studies throughout southern California and elsewhere to provide relative age estimates for geomorphic surfaces where no independent age control exists (e.g., Harden and Matti, 1989; Kendrick and McFadden, 1996). These studies have relied on the chronofunction concept. Within a series of soils composing a chronofunction, the major soil-forming factor that varies is time, as described by Jenny (1941). Properties that have been used as indicators of the duration of pedogenesis include, but are not limited to, clay accumulation (Birkeland, 1999), accumulation of $CaCO_3$ (Gile et al., 1966), and Fe oxide content and composition (Alexander, 1974; McFadden and Hendricks, 1985). Field properties, combined into an index (e.g., Harden, 1982) and an index of reddening have also been used as an indication of duration of pedogenesis (Torrent et al., 1980b). Pedogenic silica accumulation has been classified into developmental stages on a qualitative basis (Taylor, 1986; Harden et al., 1991).

Opaline silica commonly occurs as a pedogenic compound in soils of both arid and Mediterranean climatic regimes, and can ultimately form well-developed duripans (Flach et al., 1969; Norton, 1994). The source of this secondary silica is the weathering of either volcanic glass or primary silicate minerals. The optimal conditions for precipitation of silica are pH values <7, high available surface area in the soil fabric, and high ionic strength of the soil solution (Chadwick et al., 1987). In Mediterranean climatic regions where the soils lack $CaCO_3$, two of these three conditions are met. Soils of these regions often have pH values <7 and an argillic horizon relatively enriched with Fe oxides, providing a high surface area that favors silica precipitation.

A long duration of pedogenesis is required for silica cementation sufficient to form a duripan in Mediterranean regions, particularly in the absence of volcanic glass (Flach et al., 1969). Yet pedogenic silica can be an important soil component even when induration is insufficient for designation of a duripan (Marsan and Torrent, 1989; Chartres et al., 1990; Munk and Southard, 1993; Chartres and Norton, 1994; Moody and Graham, 1997). In California, silica cementation is a common phenomenon in soils developed in alluvium under semiarid Mediterranean climatic conditions. Duripans are found in soils on the oldest terraces in the Sacramento Valley, San Joaquin Valley, and southern California, but no quantitative analysis of silica as a function of age has been made. The objectives of this study were (i) to determine the usefulness of pedogenic silica as an indicator of relative age in two well-characterized soil chronosequences in southern California, and (ii) to assess potential sources of the secondary silica.

MATERIALS AND METHODS

Environmental Setting

Two soil chronosequences were used in this study. Most data are from the San Timoteo Badlands chronosequence (Kendrick and McFadden, 1996), while more limited data are presented from the nearby, but distinct, Cajon Pass chronosequence (McFadden and Weldon, 1987; Harrison et al., 1990) (Fig. 1). Soils in both settings are developed in fluvial deposits of arkosic sands and gravels, containing quartz, feldspar, and biotite as the major mineral components. Hornblende, muscovite, and magnetite are relatively minor constituents. In neither of these locations is there evidence of the influx of volcanic products. In this discussion, pedon designations from the original source data are used. Pedons labeled with the prefixes STC and RC are from the San Timoteo Badlands chrono-

K.J. Kendrick, U.S. Geological Survey, 525 S. Wilson Ave., Pasadena, CA 91106; R.C. Graham, Dep. of Environmental Sciences, Univ. of California, Riverside, CA 92521. Received 20 July 2001. *Corresponding author (kendrick@usgs.gov).

Published in Soil Sci. Soc. Am. J. 68:1295–1303 (2004).

677 S. Segoe Rd., Madison, WI 53711 USA

Abbreviations: Fe_d, dithionite-extractable Fe; Fe_o, oxalate-extractable Fe; ka, thousands of years before present; IROSL, near-infrared optical stimulation luminescence; Si_{tn}, tiron-extractable Si; TL, thermoluminescence.

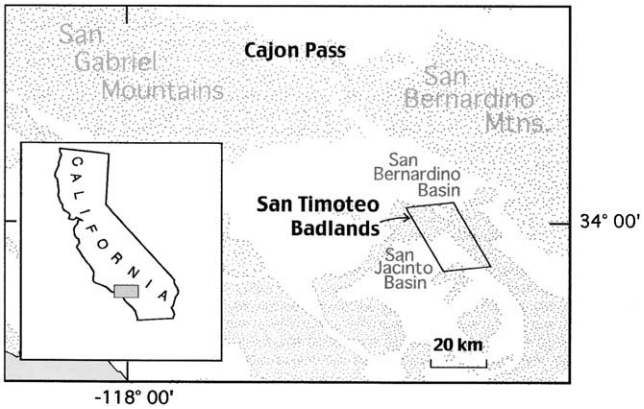

Fig. 1. Map showing the San Timoteo Badlands and nearby Cajon Pass study locations. Stippled pattern designates upland regions.

sequence, (Kendrick and McFadden, 1996), and pedons with the prefixes RW and SB are from the Cajon Pass chronosequence (McFadden and Weldon, 1987; Harrison et al., 1990) (Table 1).

The San Timoteo Badlands are immediately south of the San Bernardino Basin in southern California (Fig. 1). The mean annual air temperature in the Badlands is 17°C (thermic soil temperature regime), and the mean annual rainfall is 360 mm yr^{-1} (Clark, 1979). The climate is Mediterranean, with 60 to 70% of the rainfall occurring during the winter and essentially none during the summer (xeric soil moisture regime). The vegetation is a coastal sage scrub community (Clark, 1979), including coast sagebrush (*Artemisia californica* Less.), black sage (*Salvia mellifera* E. Greene), and white sage (*Salvia apiana* Jepson), with annual grasses. The pedons described in this area are at an elevation of between 400 and 675 m above sea level. Pedon STC 7 was sampled from an area mapped as the Greenfield series (coarse-loamy, mixed, superactive, thermic Typic Haploxeralfs), and pedons STC 6, 9, and 10 are within delineations of the Ramona series (fine-loamy, mixed, superactive, thermic Typic Haploxeralfs) (Woodruff, 1978). Pedons RC 2 and 6 are within delineations of the Monserate series (fine-loamy, mixed, superactive, thermic Typic Durixeralfs) (Knecht, 1971).

The Cajon Pass chronosequence, defined by McFadden and Weldon (1987), lies approximately 45 km to the north–northwest of the Badlands, at the eastern end of the San Gabriel Mountains. The climate in Cajon Pass is similar to that in the San Timoteo Badlands, except that the mean annual precipitation is 630 to 730 mm yr^{-1} (Ahlborn, 1982). The described pedons are at 710 to 950 m above sea level. The vegetation is dense chaparral, including chamise (*Adenostoma fasciculatum* Hook & Arn.), manzanita (*Arctostaphylus glauca* Lindley), and scrub oak (*Quercus dumosa* Nutt.). Only a reconnaissance soil survey has been published for this area and soils represented by Pedon SB 1 are included within a delineation of Xerofluvents and Xerorthents (Cohn and Retales, 1992); soils represented by Pedon RW11 have not been mapped.

Study Area Geomorphology and Age Relationships

San Timoteo Badlands Chronosequence

The San Timoteo Badlands contain two major drainages, Reche Creek and San Timoteo Creek (Fig. 2), tributaries to the Santa Ana River to the north. This study includes three geomorphic surfaces within the San Timoteo Badlands area (Morton, 1978a, 1978b, 1978c; Kendrick and McFadden, 1996). For the purposes of this discussion, geomorphic surfaces are considered to be mappable landscape elements formed during a discrete time period, after the definition of Ruhe (1956). The oldest surface (Q3, Fig. 2) is widespread and has been incised by the developing San Timoteo and Reche drainages. Younger surfaces (Q1, Q2, Fig. 2) are inset within both Reche and San Timoteo canyons. The inset surfaces slope toward the axial stream, and are interpreted as being aggradational surfaces associated with tributary streams.

Tentative age estimates were assigned to the surfaces in the San Timoteo Badlands (Table 2) based on correlations of soil development indices (Harden, 1982; Harden and Taylor, 1983; Torrent et al., 1980b) with those of nearby, dated chronosequences (Kendrick and McFadden, 1996). The age estimates have been refined, using luminescence dating and paleomagnetic correlation to provide independent age determinations of the associated sediments (Kendrick, 1999). The oldest surface (Q3) was assigned broad age estimates of 300 to 700 ka based on correlation with dated chronosequences. Correlation of the deposits beneath this surface with the Magnetic Polarity Time Scale (Albright, 1997) confirms that the preferred age (approximately 500 ka) for the formation of this surface is reasonable (Kendrick, 1999).

Thermoluminescence (TL) and near-infrared optical stimulation luminescence (IROSL) dating of the sediments underlying the pedon associated with surface Q2 yielded an age range of 64 $\pm$ 5 ka at 2.3 m below the surface (Table 2). This age estimated for the sediments implies that the stabilization of the surface, and the accompanying inception of pedogenesis occurred at some time after 64 $\pm$ 5 ka.

The youngest surface, Q1, is located in the northern part of the San Timoteo drainage. The TL and IROSL dating indicated a mean age ranging from 47.2 to 59.2 ka for sediments collected within 5 m of the surface (Table 2). The stabilization of the surface occurred at sometime after the deposition of these sediments.

Cajon Pass Chronosequence

The Cajon Pass chronosequence was defined by McFadden and Weldon (1987) on a flight of 11 fluvial terraces associated with Cajon Creek. Ages were determined using paleomagnetic, radiometric, and inferential methods. The surface Qoad was determined to be approximately 55 ka, based on the comparison with older and younger dated surfaces, and the extrapolation of a constant slip rate along the San Andreas fault (McFadden and Weldon, 1987). The age for surface Qoac, 11.5 ka, was determined by radiocarbon dating of the underlying sediments (McFadden and Weldon, 1987).

Field and Laboratory Methods

Thorough morphologic descriptions (Soil Survey Staff, 1951, 1999; Birkeland, 1999) were made of 22 pedons on the three geomorphic surfaces in the San Timoteo Badlands (Kendrick, 1993; 1996; Kendrick and McFadden, 1996). Based on these preliminary studies, representative pedons from each surface (STC 7 on Q1; STC 9, RC 6 on Q2; STC 10, STC 6, RC 2 on Q3) were selected for more detailed analysis (Fig. 2, Table 1). In addition, two pedons (RW 11 on Qoad; and SB 1 on Qoac) from Cajon Pass (Table 1; McFadden and Weldon, 1987; Harrison et al., 1990) were included in this study to compare results from a second chronosequence. In all cases, bulk samples were taken from morphologic horizons exposed in freshly excavated pits. When horizons exceeded 75 cm in thickness (Btqm2 of STC 6 and Btqm3 of RC 2), the horizons were subdivided for sampling and subsequent analysis.

In the laboratory, soil samples were air-dried and sieved

Table 1. Properties of representative pedons in the Cajon Pass chronosequence (SB, RW) and the San Timoteo Badlands chronosequence (STC, RC).

Horizon	Depth	Color		Texture†	Structure‡	Dry consistence§	Clay films¶
		Dry	Moist				
	cm	Cajon Pass					
		SB1 (Qoac, 11.5 ka): sandy, mixed, thermic Typic Haploxeralf††					
A1	0–3	10YR4/2	10YR2/2	LS	lfgr	so	0
A2	3–20	10YR5/3	10YR3/3	LS	lmsbk	sh	0
2Bt1	20–50	10YR6/4	10YR4/3	LS	2csbk	h	2nco
3Bt2	50–85	2.5Y6/4	2.5Y4/4	LS	2csbk	h	2nco
3Cox‡‡	85–110	2.5Y6/4	2.5Y4/3	S	sg	lo	0
		RW11 (Qoad, 55 ka): coarse-loamy, mixed, superactive, thermic Typic Haploxeralf§§¶¶					
O1	7–0						
BA	0–9	7.5YR5/3	7.5YR3/4	SL	3msbk	h	1npo,co
2Bt1	9–42	5YR4/6	5YR4/4	gL	2msbk	h	2npo,co,br
2Bt2	42–77	5YR5/6	5YR4/4	gSCL	2f,msbk	h	2mkpo,br,co
2Bt3	77–99	6.3YR5/4	6.3YR4/4	gSL	m	h	1mkpo,br,co
2BC	99–140	7.5YR6/6	7.5YR4/6	gLS	m	so	co
2Cox1	140–190	8.8YR6/4	8.8YR4/4	gCOS	sg	lo	0
2Cox2	190+	10YR7/4	10YR4/4	gCOS	sg	lo	0
		San Timoteo Badlands					
		STC 7 (Q1, 47 ka): fine-loamy, mixed, superactive, thermic Typic Argixeroll##					
A	0–28	10YR5/3	10YR3/3	SL	1fsbk	so-sh	0
AB	28–38	10YR5/4	10YR4/3	SL	2msbk	sh	1vnpf
Bt1	38–90	7.5YR–10YR5/5	7.5YR4/4	SL	3msbk-pr	h	1mkpf, 2nbr
2Bt2	90–120	10YR6/4	10YR4/4	SL	2mbsk	h-vh	1mkpf
2Bt3	120–167	10YR6/3	10YR4/4	SL	1msbk	h-vh	v1nco
3CB	167–200	10YR7/4	10YR5/4	SL	2msbk-abk	vh	0
		STC 9 (Q2, 55 ka): coarse-loamy, mixed, superactive, thermic Typic Haploxeralf§§##					
Bt1	0–18	7.5YR4.5/4	7.5YR4/4	L	2csbk	h	v1mkpf, 1nbrpf
2Bt2	18–54	7.5YR5/4	7.5YR4/4	SL	3msbk	sh-h	1mkpf, 1nbr,pf
3Bt3	54–80	10YR6/6	7.5YR4/4	SL	3fsbk	vh	1npf,br
3BC	80–108	10YR6/4	7.5YR4/4	SL	3mbsk	vh	1npf,br
3CB	108–120	10YR6/4	10YR5/4	LS	2msbk	vh	0
		RC 6 (Q2, 55 ka): coarse-loamy, mixed, superactive, thermic Typic Argixeroll##					
Ap	0–34	10YR4/3	10YR3/3	SL	1msbk	vsh	0
AB	34–80	10YR5/4	10YR4/3	SL	1msbk	sh	1npf
Bt1	80–129	7.5YR5/6	7.5YR4/6	SL	2msbk	h	2mkpf,1nbr
Bt2	129–155	7.5YR6/6	7.5YR5/6	SL	2msbk	h	1mkpf,1npf
BC	155–178	10YR6/4	10YR5/4	SL	1msbk-abk	sh-h	1npf
2Cox/Bt	178–225	10YR6/5	10YR5/4	LS	sg,v1fsbk	sh	1npf
2Cox2	225–297	10YR6/3	10YR5/3	LS	sg,v1fsbk	so	0
3Bt1b	297–333	10YR5/4	10YR5/4	SL	2fabk	sh	2npf
3Bt2b	333–383	10YR4/4	10YR4/4	LS	2fabk	sh-h	2npf
		STC 10 (Q3, 500 ka): coarse-loamy, mixed, superactive, thermic Typic Durixeralf§§##					
Btqm1	0–35	2.5YR4/6	5YR4/6	SL	3mbsk	vh	1kpf,2nbr,2mkpf
Btqm2	35–89	7.5YR4.5/6	6.25YR5/6	SL	2mbsk	h	1mkpf,2nbr
Cox	89–115	10YR5/4	10YR4/4	SL	1mbsk	sh	0
		RC 2 (Q3, 500 ka): sandy, mixed, thermic Typic Durixeralf§§##					
Bt1m1	0–45	5YR4/6 5YR5/8	5YR5/8	S	3cpr	h	2kpf,1nbr
Btqm2	45–61	7.5YR5/8 7.5YR4/6	7.5YR5/6	LS	2mbsk	h	2npf,br,v1kpf
Btqm3	61–230	7.5YR5/4–6	7.5YR4/6	LS	2msbk	h	1npf
BCtq	230–235	10YR5/4	10YR4/4	LS	m	vh	0
		STC 6 (Q3, 500 ka): fine-loamy, mixed, superactive, thermic Typic Durixeralf§§##					
Btqm1	0–35	2.5YR4/8	2.5YR4/7	SCL	3cabk	vh	2kpf,4nbr
Btqm2	35–111	5YR5/6	3.75YR4/6	SL	3cabk	vh	1kpf,3nbr
Btq	111–185	7.5YR5/7	7.5YR4/6	LS	2csbk	sh,h#	1nbr,v1mkbr#
BCtq	185–225	7.5YR5/6	7.5YR4/6	S	1msbk	sh	0

† COS, coarse sand; L, loam; LS, loamy sand; S, sand; SC, sandy clay; SCL, sandy clay loam; SICL, silty clay loam; SIL, silt loam; SL, sandy loam; g, gravelly.
‡ 1 = weak; 2 = moderate; 3 = strong; f, fine; m, medium; c, coarse; v, very; gr, granular; sbk, subangular blocky; abk, angular blocky; pr, prismatic; m, massive; sg, single grain.
§ lo, loose; so, soft; sh, slightly hard; h, hard; vh, very hard.
¶ 0 = none; 1 = few; 2 = common; 3 = many; 4 = continuous; n, thin; mk, moderately thick; k, thick; v, very; pf, ped faces; po, pores; br, bridging grains; co, colloidal stains.
# Consistence and clay films for Bt bands.
†† Pedon description previously published in Harrison et al. (1990).
‡‡ Cox horizon designation after Birkeland (1999).
§§ Pedons RW11, STC 9, STC 10, RC 2, and STC 6 have been truncated by erosion so that B horizons are exposed at the surface.
¶¶ Pedon description previously published in Weldon (1987).
Pedon descriptions previously published in Kendrick and McFadden (1996).

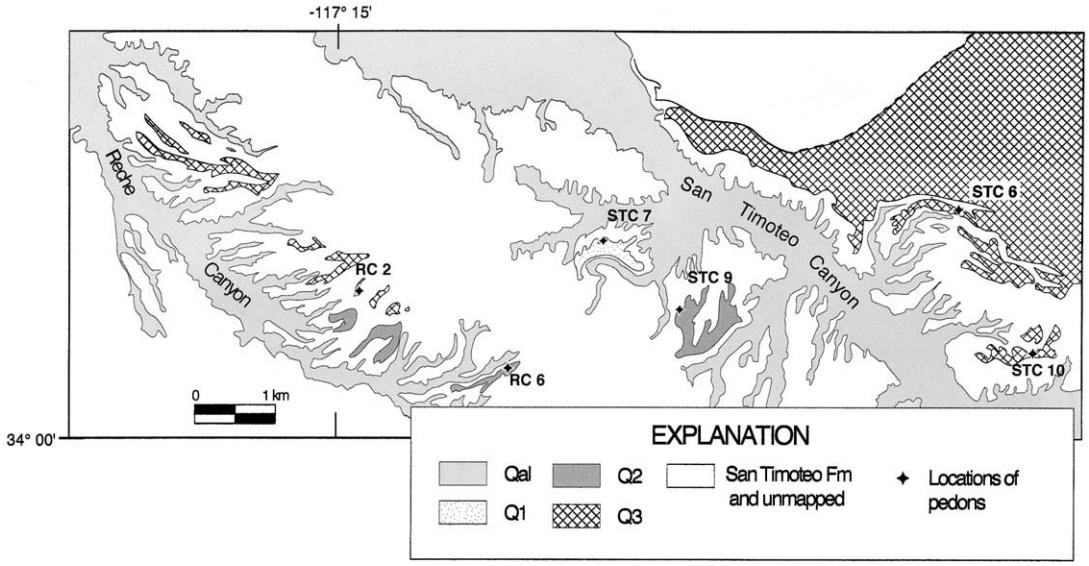

Fig. 2. Map of the San Timoteo study area, showing San Timoteo and Reche drainages, geomorphic surfaces (Q1, Q2, Q3), and location of pedons. The STC and RC designations refer to the pedons described on surfaces within the San Timoteo and Reche drainages, respectively.

to remove rock fragments >2 mm in diameter. Particle-size distribution was measured by wet sieving and pipette (Gee and Bauder, 1986).

Quantification of pedogenic opaline silica relies on selective dissolution techniques. The most common method used is hot sodium hydroxide extraction, which primarily attacks amorphous and poorly ordered silica, but also fine-grained crystalline clays (Kodama and Ross, 1991). Kodama and Ross (1991) concluded, based on laboratory extractions of natural and synthetic standards, that the tiron (4,5-dihydroxy-1,3-benzenedisulfonic acid [disodium salt], $C_6H_4Na_2O_8S_2$) extraction method successfully extracted the secondary silica without affecting the crystalline compounds. The tiron extraction technique is thus the most effective method of quantifying pedogenic silica and is used in this study. The extraction for this study follows the method of Kodama and Ross (1991), modified from the original method of Biermans and Baert (1977). An aqueous solution of tiron, with a pH of about 5.5, was adjusted to pH 10.2 with a Na_2CO_3 solution. The pH was brought to 10.5 by adding 4 *M* NaOH. A final concentration of 0.1 *M* tiron was achieved. A 30-mL aliquot of this tiron solution was added to 25 mg of dry, ground soil material (<100 mesh) and heated in a 80°C water bath for 1 h. The samples were then cooled, weighed, and water added to account for any evaporation. The samples were centrifuged, and finally, the supernatant was analyzed for extracted Si by atomic absorption spectroscopy.

Total elemental composition was determined by fusing 0.2 g of sieved, <2-mm soil material with 1.2 g of $LiBO_2$, followed by dissolution in 100 mL of 1.1 *M* HNO_3, and measurement by inductively coupled argon plasma spectroscopy (Ingamells, 1970).

For one pedon, STC 6, fine sands treated with citrate-bicarbonate-dithionite (Jackson et al., 1986) were mounted in immersion oil with a refractive index of 1.544 and 100 grains were counted by line transecting using a petrographic microscope. Magnesium- and K-saturated clay samples from the same pedon were smeared on glass slides for X-ray diffraction analysis, employing Cu-Kα radiation, a graphite crystal monochromator, and a scintillation counter. In addition, thermogravimetric analysis was performed on Na-saturated, freeze-dried clays and weight percentages of kaolinite were calculated using a standard composed of halloysite and poorly crystalline kaolinite (Halloysite no. 29, Ward's Natural Science Establishment, Inc., Rochester, NY).

Table 2. Ages of geomorphic surfaces in the San Timoteo Badlands as determined by soil correlation, luminescence (thermoluminescence [TL] and near-infrared optical stimulation luminescence [IROSL]), and paleomagnetic analysis. Age determinations by luminescence are 1σ uncertainty values for these samples from the upper 5 meters. Sample numbers as reported in Kendrick, 1999.

Surface	Soil correlation age	TL age	IROSL age	Paleomagnetic analysis
	ka			
Q1	27.5–67	47.2 ± 9.7†	59.2 ± 3.4‡	
Q2	43–67		84.6 ± 9.0§	
			64.0 ± 5.4¶	
Q3	300–700			<780 ka

† Sample # STC TL-14.
‡ Sample # STC TL-1.
§ Sample # STC TL-23.
¶ Sample # STC TL-33.

RESULTS AND DISCUSSION

Soil Morphology

All of the intact pedons examined in this study have clay distributions that meet argillic horizon criteria, although maximum clay contents increase from 10% in the youngest soil (SB1, 11.5 ka) to 24% in the one of the oldest (STC 6, 500 ka) (Fig. 3). All of the 500-ka soils and one of the 55-ka soils (STC 9) have been truncated by erosion so that Bt horizons are exposed at the surface. For these soils, an argillic horizon was interpreted based on clay films and clay distributions in the remnant profiles. These soils (STC 6, RC 2, STC 10, STC 9), as well as the youngest soil (SB1), have ochric epipedons and are Alfisols, whereas the two remaining intermediate-age soils (STC 7, RC 6) have mollic epipedons and are Mollisols (Table 1). More thorough discussions of soil particle-size distributions, pedogenic Fe oxides, and various field-determined morphologic properties have been previ-

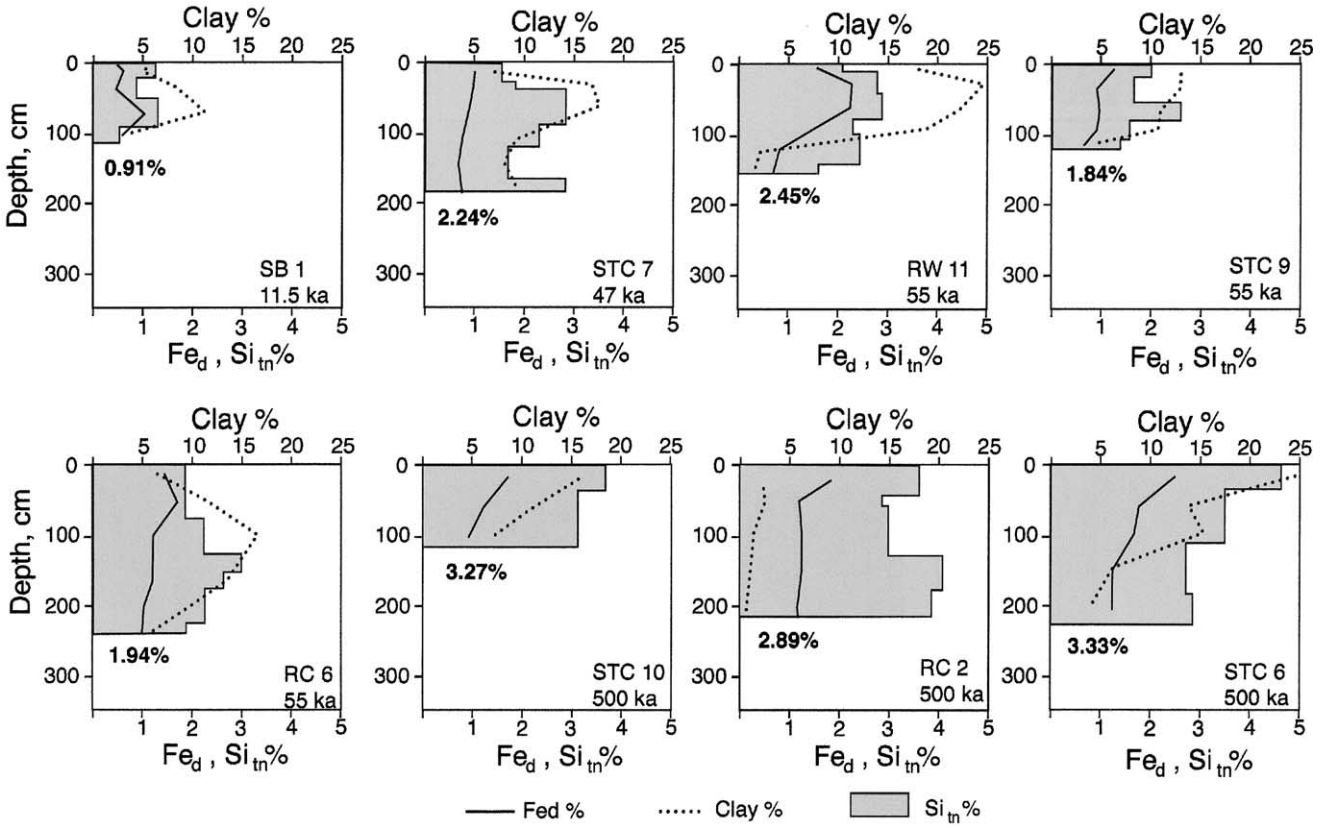

Fig. 3. Depth plots showing pedogenic silica content (shaded regions) in the studied pedons. The numerical value in each plot indicates the depth-weighted average of secondary silica. The silica content was integrated to a depth of 20 cm into the C or Cox horizon for each pedon (Table 1). The Fe_d (citrate-bicarbonate-dithionite-extractable Fe; solid lines) and percentage of clay (dotted lines) are plotted for comparison (data from Kendrick and McFadden, 1996).

ously presented for RW 11 (McFadden and Weldon, 1987), SB1 (Harrison et al., 1990), and the San Timoteo Badlands soils (Kendrick and McFadden, 1996).

The soils that are 55 ka and younger have no visible silica precipitation in any part, but individual peds have hard to very hard rupture resistance. The nearly vertical slopes at the natural edges of the surfaces suggest cementation of some kind imparts strength to these materials. Similar vertical scarps on marine terraces on the central California coast were caused by silica cementation (Moody and Graham, 1997). On the Q3 surface (500 ka), soils vary from having no macroscopic pedogenic silica features to those having weakly expressed duripans with discontinuous opal coatings on the faces of very coarse prisms (0.5- to 2-m diam.) and within widely spaced fractures that cut diagonally across the prisms. The Q3 soils used in this study (STC 6, RC 2, STC 10) did not have macroscopically visible pedogenic silica features, but micromorphological observations revealed opaline silica coatings on ferriargillans, along ped faces, and within pores (Kendrick, 1996). Fragments of Bt horizons from the Q3 surface did not slake in water, whereas those from younger surfaces did.

Secondary Silica

All of the soils contained Si_{tn} within the <2-mm fraction, with maximum horizon values for each pedon ranging from about 1.2 to 4.6% (Fig. 3). These values are comparable with those reported for duripans and/or Btqm horizons on a southern California marine terrace (1.64% Si_{NaOH}; Torrent et al., 1980a), at a marine terrace edge in central California (3.58% Si_{tn}; Moody and Graham, 1997), on a granitic pediment in the Mojave Desert, California (4.24% Si_{NaOH}; Boettinger and Southard, 1991), and in mixed volcanic and eolian materials in central Nevada (2.24% Si_{NaOH}; Chadwick et al., 1987). Both the maximum horizon Si_{tn} value (Fig. 3) and the profile weighted mean value (Fig. 4a) increase with increasing soil age, reflecting the progressive accumulation of pedogenic silica. While maximum expression of silica accumulation, in the form of duripans, is usually associated with ancient surfaces or soils derived from volcanic glass (Flach et al., 1969; Chadwick et al., 1989), our data show silica accumulation in an area with no known volcanic glass, and in soils as young as about 11.5 ka (SB1 on Qoac; Fig. 3 and 4a).

The depth profiles of Si_{tn} show that maximum values generally coincide with the strongest expression of the B horizon, as indicated by clay and Fe_d distributions (Fig. 3; Kendrick and McFadden, 1996). The clay contents of these soils may be higher than the values reported in Fig. 3 if silica cementation inhibited dispersion. The greater surface area provided by the increased clay content in these horizons likely promotes the precipitation of silica, as proposed by Chadwick et al. (1987). Iron oxides can serve as a template for the adsorption of $Si(OH)_4$ (Marsan and Torrent, 1989).

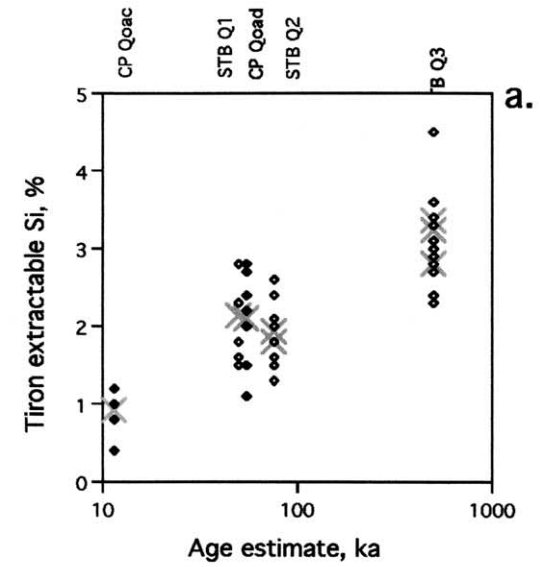

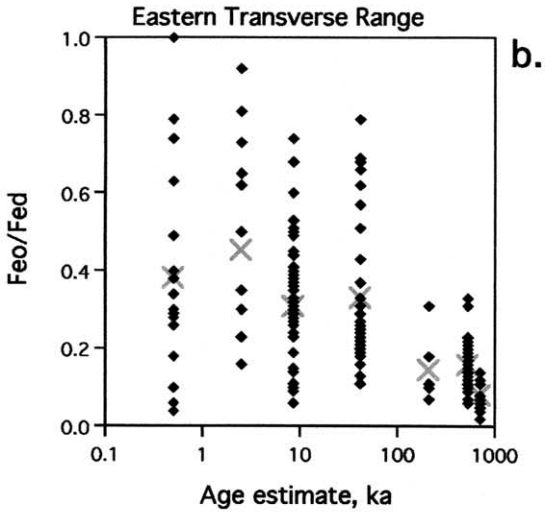

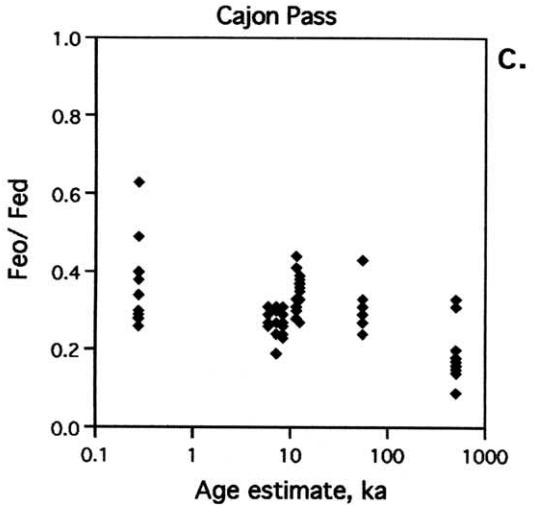

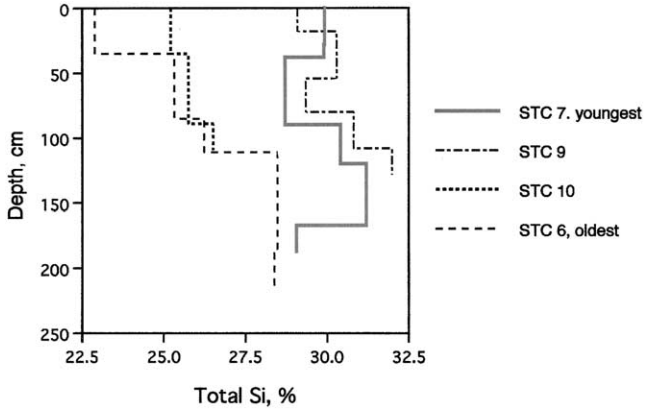

Fig. 5. Depth plots showing primary Si as a function of age for the <2-mm fraction of soils in San Timoteo Canyon.

The good agreement in Si_{tn} values between soils having similar development and age in the two different chronosequences, Cajon Pass and in the San Timoteo Badlands (CP Qoad and STB Q1, Q2; Fig. 4a), suggests that the accumulation of secondary silica may be a valuable indication of soil age. Although there is a range of Si_{tn} values for soils of each age (Fig. 4a), this is also true for other methods used to assess the duration of pedogenesis, such as Fe_o/Fe_d ratios (Fig. 4b,c). The variability in the Fe_o/Fe_d ratios for alluvial terrace soils of the eastern Transverse Range (Fig. 4b; McFadden, 1982) is in part due to the wide range of estimated ages for these soils. In the Cajon Pass chronosequence (Fig. 4c), the uncertainty associated with the age estimates is less, a result of better age control (McFadden and Weldon, 1987). The degree of uncertainty in the ages for the San Timoteo Badlands chronosequence soils is similar to the age uncertainty of those at Cajon Pass, allowing a more direct comparison of the two methods. The Si_{tn} approach compares very favorably with the Fe_o/Fe_d method, both in terms of variability within a given age category and for showing a trend with increasing soil age.

Sources of Silica

The general pattern of decrease in primary Si (Si_T less Si_{tn}) with increasing age (Fig. 5) demonstrates the progressive weathering of the primary minerals and

Fig. 4. Graphs showing variability associated with chronosequence analysis. (a) Plot of the relation between age estimate (ka) and horizon values of tiron-extractable Si (%) for pedons in Cajon Pass (CP) and San Timoteo Badland (STB) study areas. The results are arranged by surface, with the designation of CP or STB as modifiers to the surface designation (i.e., CP Qoac is the Qoac surface in Cajon Pass). The values for the Cajon Pass horizons are shown with a closed diamond, while San Timoteo soil horizon values are shown using an open diamond. Mean values for each pedon (sometimes more than one per surface) are plotted with a large "X" symbol. The data shown for each surface are from the following pedons: Surface CP Qoac: Pedon SB1; Surface STB Q1: Pedon STC 7; Surface CP Qoad: Pedon RW 11; Surface STB Q2: Pedons STC 9, RC 6; Surface STB Q3: Pedons RC 2, STC 10, STC 6. (b) Horizon values of Fe_o/Fe_d ratios for the soils in the Eastern Transverse Range chronosequence (McFadden, 1982; McFadden and Hendricks, 1985). (c) Horizon values of Fe_o/Fe_d ratios for the Cajon Pass chronosequence (McFadden and Weldon, 1987).

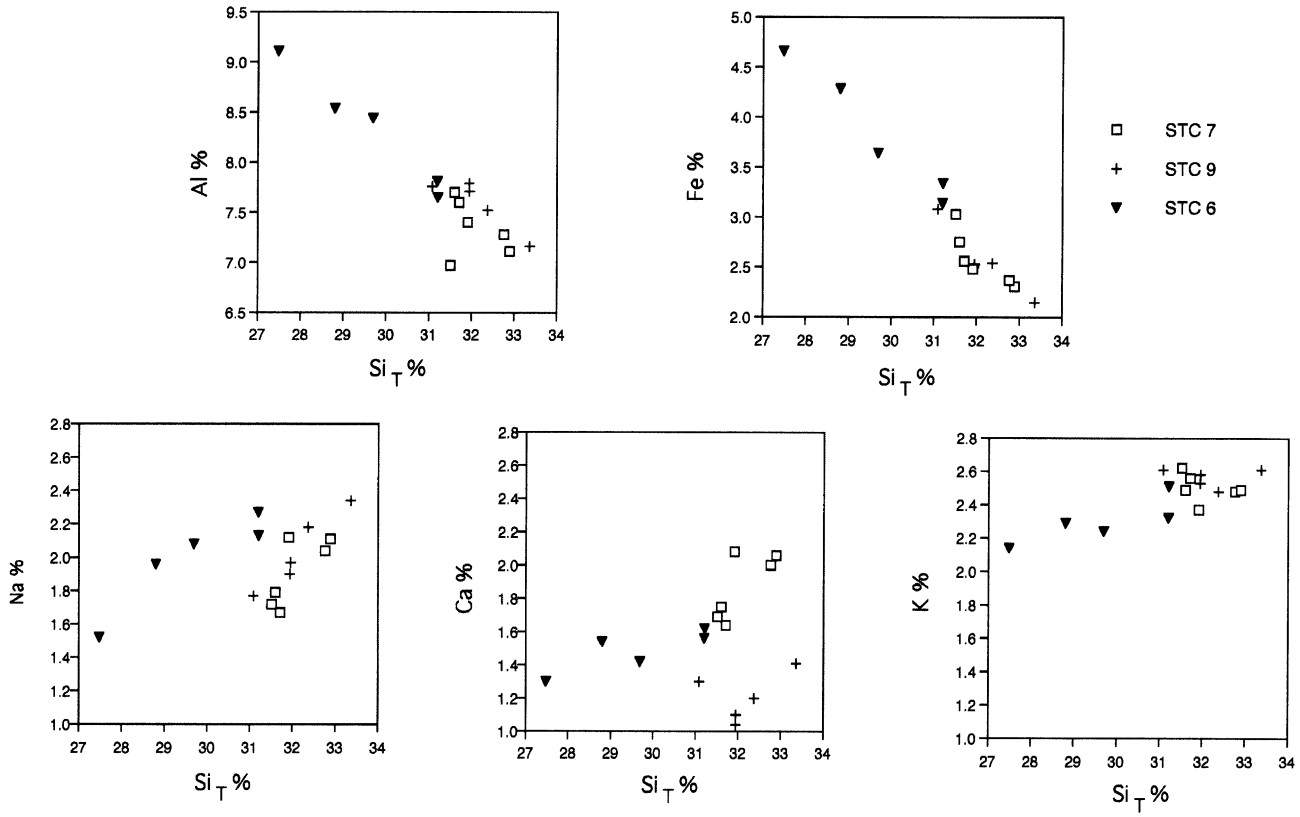

Fig. 6. Plots of elements (K, Na, Ca, Fe, Al) versus Si from total elemental analysis of <2-mm fraction of horizons from STC pedons. Tabulated values are available in Kendrick (1999). Approximate surface ages are: STC = 47 ka; STC9 = 55 ka; STC6 = 500 ka.

leaching of soluble Si from the pedon. More primary Si is leached from the upper horizons (Fig. 5) because weathering intensity and water flux is greatest in that zone. Conditions that enhance Si solubility (dissolution) prevail in the upper horizons, specifically the presence of organic material, low ionic strength (atmospheric) water, and frequent wetting-and-drying cycles (Baker and Schrivner, 1985). The depletion in the uppermost horizons is on the order of 1 to 5 weight percentage of Si. Iron and Al are conserved in the profiles relative to Si, and, as a result, become concentrated as Si is depleted (Fig. 6). Iron released by weathering is retained as oxides (Kendrick and McFadden, 1996; McFadden and Weldon, 1987), and released Al is retained in kaolin and is commonly substituted into Fe oxides (Bigham et al., 2002). On the other hand, Na, Ca, and especially K, are depleted concurrent with losses of Si in the oldest soil, STC 6 (Fig. 6). The trend is less obvious for the younger pedons, STC7 and STC9, because less Si has been lost via weathering, resulting in a narrow range of Si values.

Petrographic and X-ray diffraction analysis showed that the fine sand-size (0.10–0.25 mm) fraction of the B and C horizons of the STC 6 pedon consists of primarily quartz, albite, orthoclase, and biotite, with lesser amounts of hornblende, randomly interstratified biotite/vermiculite, and magnetite. The clay fraction (<2 μm), as determined by X-ray diffraction, consisted of vermiculite, kaolin, biotite, and randomly interstratified biotite/vermiculite. These suites of minerals are typical of soils formed in granitic-derived regoliths of southern California (Nettleton et al., 1968; Tice et al., 1996; Frazier and Graham, 2000). Thermogravimetric analysis indicated that the kaolin comprised 50 to 60% of the clay fraction. Vermiculite is the weathering product of biotite, with K and, to a lesser extent, Fe released in the transformation (Douglas, 1989). Weathering of the feldspars in the STC 6 pedon presumably yields kaolin, with Na, K, and Si released during this process (Birkeland, 1999). Silicon is also released by weathering of the other aluminosilicate components of this soil, such as hornblende.

The primary Si loss in the studied pedons is approximately equivalent to the accumulation of opal Si, suggesting that the weathering of primary minerals is an adequate source for this secondary silica in these soils (Fig. 3, 5). As an example, STC 6 shows a 5.48% weight loss of primary Si, as compared with a 4.58% gain of opal Si in the uppermost horizon (Btqm1), and a 3.06% loss of primary Si and a gain of 3.48% opal Si in the next lower horizon (Btqm2) (Fig. 3, 5). This comparison cannot be made with precision because the loss of primary Si is determined in relation to lower horizons that may not accurately represent the parent material (e.g., BCtq in Pedon STC 6), and have experienced an uncertain degree of weathering. In addition, the stripping of the uppermost horizons from these pedons has removed material that probably functioned as a source of opal Si for the deeper horizons. The loss of primary Si in the missing horizons cannot be evaluated. Both of these uncertainties would contribute to an underestimation of the loss of primary Si and potential production of

opal Si. Nevertheless, the calculated loss of primary Si approximates gains in opal Si, suggesting that weathering of the arkosic sediment could serve as the source of opal Si. Torrent et al. (1980a) were similarly able to demonstrate that Si released by the weathering of primary minerals in upper horizons was more than adequate to account for silica accumulated in the underlying duripan in coastal southern California.

CONCLUSIONS

There is an overall, progressive loss of primary Si in the studied chronosequence soils. The Si loss is concurrent with the loss of K and Na, and likely reflects the dissolution of feldspar minerals. Pedogenic silica increases with increasing soil age in both the San Timoteo and Cajon Pass chronosequences. The release of Si from primary mineral weathering, particularly K and Na feldspars, is adequate to account for the amount of secondary silica accumulation. The amount of pedogenic silica in soils in the San Timoteo study area is consistent with similarly developed soils in the Cajon Pass chronosequence. Although the pedons described in these two chronosequences did not contain macroscopically visible opaline silica, selective dissolution data show secondary silica in soils as young as 11.5 ka. Pedogenic silica extracted with tiron correlated to chronosequential age estimates with a variability comparable with that obtained with the Fe_o/Fe_d method. Tiron-extractable Si promises to be a useful indicator of soil age in environments conducive to duripan formation.

ACKNOWLEDGMENTS

The authors thank Kathy Rose for assistance with the analysis of pedogenic silica, Brad Lee for mineralogical data, and Les McFadden and Bruce Harrison for access to Cajon Pass samples.

REFERENCES

Ahlborn, W.O. 1982. Santa Ana River Basin flood hazard. San Bernardino County Museum Q. 29:1–95.

Albright, L.B. 1997. Geochronology and vertebrate paleontology of the San Timoteo badlands, southern California. Ph.D. diss. Univ. of California, Riverside.

Alexander, E.B. 1974. Extractable iron in relation to soil age on terraces along the Truckee River, Nevada. Soil Sci. Soc. Am. Proc. 38:121–124.

Baker, J.C., and C.L. Schrivner. 1985. Simulated movement of silicon in a Typic Hapludalf. Soil Sci. 139:255–261.

Birkeland, P.W. 1999. Soils and geomorphology. Oxford University Press, New York.

Biermans, V. and L. Baert. 1977. Selective extraction of the amorphous Al, Fe, and Si oxides using an alkaline tiron solution. Clay Miner. 12:127–135.

Bigham, J.M., R.W. Fitzpatrick, and D.G. Schulze. 2002. Iron oxides. p. 323–366. *In* J.B. Dixon and D.G. Schulze (ed.) Soil mineralogy with environmental applications. SSSA Book Ser. 7. SSSA, Madison, WI.

Boettinger, J.L., and R.J. Southard. 1991. Silica and carbonate sources for Aridisols on a granitic pediment, western Mojave Desert. Soil Sci. Soc. Am. J. 55:1057–1067.

Chadwick, O.A., D.M. Hendricks, and W.D. Nettleton. 1987. Silica in duric soils: I. A depositional model. Soil Sci. Soc. Am. J. 51:975–982.

Chadwick, O.A., D.M. Hendricks, and W.D. Nettleton. 1989. Silicification of Holocene soils in Northern Monitor Valley, Nevada. Soil Sci. Soc. Am. J. 53:158–164.

Chartres, C.J., J.M. Kirby, and M. Raupach. 1990. Poorly ordered silica and aluminosilicates as temporary cementing agents in hardsetting soils. Soil Sci. Soc. Am. J. 54:1060–1067.

Chartres, C.J., and L.D. Norton. 1994. Micromorphological and chemical properties of Australian soils with hardsetting and duric horizons. Dev. Soil Sci. 22:825–834.

Clark, A.O. 1979. Quaternary evolution of the San Bernardino Valley. Q. San Bernardino County Museum Assoc. 26:1–150.

Cohn, B.R., and J.G. Retales. 1992. Soil survey of San Bernardino National Forest area, California. U.S. Gov. Print. Office, Washington, DC.

Douglas, L.A. 1989. Vermiculites. p. 635–674. *In* J.B. Dixon and S.B. Weed (ed.) Minerals in soil environments. 2nd ed. SSSA Book Ser. No. 1. SSSA, Madison, WI.

Flach, K.W., W.D. Nettleton, L.H. Gile, and J.G. Cady. 1969. Pedocementation: Induration by silica, carbonates and sesquioxides in the Quaternary. Soil Sci. 107:442–453.

Frazier, C.S., and R.C. Graham. 2000. Pedogenic transformation of fractured granitic bedrock, southern California. Soil Sci. Soc. Am. J. 64:2057–2069.

Gee, G.W., and J.W. Bauder. 1986. Particle-size analysis. p. 383–411. *In* A. Klute (ed.) Methods of soil analysis. Part 1. 2nd. ed. Agron. Monogr. 9. ASA and SSSA, Madison, WI.

Gile, L.H., F.F. Peterson, and R.B. Grossman. 1966. Morphological and genetic sequences of carbonate accumulations in desert soils. Soil Sci. 101:347–360.

Harden, J.W. 1982. A quantitative index of soil development from field descriptions: Examples from a chronosequence in central California. Geoderma 28:1–28.

Harden, J.W., and E.M. Taylor. 1983. A quantitative comparison of soil development in four climatic regimes. Q. Res. 20:342–359.

Harden, J.W., and J.C. Matti. 1989. Holocene and late Pleistocene slip rates on the San Andreas fault in Yucaipa, California, using displaced alluvial-fan deposits and soil chronology. Geol. Soc. Am. Bull. 101:1107–1117.

Harden, J.W., E.M. Taylor, M.C. Reheis, and L.D. McFadden. 1991. Calcic, gypsic and siliceous soil chronosequences in arid and semiarid environments. p. 1–16. *In* W.D. Nettleton (ed.) Occurrence, characteristics, and genesis of carbonate, gypsum, and silica accumulations in soils. SSSA Spec. Publ. 26. SSSA, Madison, WI.

Harrison, J.B.J., L.D. McFadden, and R.J. Weldon. 1990. Spatial soil variability in the Cajon Pass chronosequence: Implications for the use of soils as a geochronologic tool. Geomorphology 3:399–416.

Ingamells, C.O. 1970. Lithium metaborate flux in silicate analysis. Anal. Chim. Acta 52:323–334.

Jackson, M.L., C.H. Lim, and L.W. Zelazny. 1986. Oxides, hydroxides, and aluminosilicates. p. 101–150. *In* A. Klute (ed.) Methods of soil analysis. Part 1. 2nd. ed. Agron. Monogr. 9. ASA and SSSA, Madison, WI.

Jenny, H. 1941. Factors of soil formation. McGraw-Hill, New York.

Kendrick, K.J. 1993. Soil development in the northern part of the San Timoteo Badlands, San Bernardino and Riverside Counties, California. M.S. thesis. Univ. of New Mexico, Albuquerque.

Kendrick, K.J. 1996. Descriptions and laboratory analysis for soils in the southern San Timoteo Badlands Area, California. U.S. Geol. Surv. Open-File Report 96–93. U.S. Geological Survey, Reston, VA.

Kendrick, K.J. 1999. Quaternary geologic evolution of the northern San Jacinto fault zone: Understanding evolving strike-slip faults through geomorphic and soil stratigraphic analysis. Ph.D. diss. Univ. of California, Riverside.

Kendrick, K.J., and L.D. McFadden. 1996. Comparison and contrast of processes of soil formation in the San Timoteo Badlands with chronosequences in California. Q. Res. 46:149–160.

Kodama, H., and G.J. Ross. 1991. Tiron dissolution method used to remove and characterize inorganic components in soils. Soil Sci. Soc. Am. J. 55:1180–1187.

Knecht, A.A. 1971. Soil survey of western Riverside Area, California. U.S. Gov. Print. Office, Washington, DC.

Marsan, F.A., and J. Torrent. 1989. Fragipan bonding by silica and iron oxides in a soil from northwest Italy. Soil Sci. Soc. Am. J. 53: 1140–1145.

McFadden, L.D. 1982. The impact of temporal and spatial climate

change on alluvial soils genesis in southern California. Ph.D. diss. Univ. of Arizona, Tuscon.
McFadden, L.D., and D.M. Hendricks. 1985. Changes in the content and composition of pedogenic iron oxyhydroxides in a chronosequence of soils in southern California. Q. Res. 23:189–204.
McFadden, L.D., and R.J. Weldon, R.J. 1987. Rates and processes of soil development in Cajon Pass, California. Geol. Soc. Am. Bull. 98:280–293.
Moody, L.E., and R.C. Graham. 1997. Silica-cemented terrace edges, central California coast. Soil Sci. Soc. Am. J. 61:1723–1729.
Morton, D.M. 1978a. Geologic map of the San Bernardino South quadrangle, San Bernardino and Riverside Counties, California. U.S. Geol. Surv. Open-File Report 78–20. U.S. Geological Survey, Reston, VA.
Morton, D.M. 1978b. Geologic map of the Redlands quadrangle, San Bernardino and Riverside Counties, California. U.S. Geol. Surv. Open-File Report 78–21. U.S. Geological Survey, Reston, VA.
Morton, D.M. 1978c. Geologic map of the Sunnymead quadrangle, Riverside County, California. U.S. Geol. Surv. Open-File Report 78–22. U.S. Geological Survey, Reston, VA.
Munk, L.P., and R.J. Southard. 1993. Pedogenic implications of opaline pendants in some California late-Pleistocene Palexeralfs. Soil Sci. Soc. Am. J. 57:149–154.
Nettleton, W.D., K.W. Flach, and R.E. Nelson. 1968. A toposequence of soils in tonalite grus in the southern California Peninsular Range. USDA-SCS Soil Surv. Invest. Rep. no. 21. U.S. Gov. Print. Office, Washington, DC.
Norton, L.D. 1994. Micromorphology of silica cementation in soils. Dev. Soil Sci. 22:811–824.
Ruhe, R.V. 1956. Subareal landscape evolution and soil development in a humid region. Geol. Soc. Am. Bull. 67:1730–1731.
Soil Survey Staff. 1951. Soil survey manual. USDA Agric. Handb. 18. U.S. Gov. Print. Office, Washington, DC.
Soil Survey Staff. 1999. Soil taxonomy: A basic system of soil classification for making and interpreting soil surveys. 2nd ed. USDA Agric. Handb. 436. U.S. Gov. Print. Office, Washington, DC.
Taylor, E.M. 1986. Impact of time and climate on Quaternary soils in the Yucca Mountain area of the Nevada Test Site, M.S. thesis, University of Colorado, Boulder, CO.
Tice, K.R., R.C. Graham, and H.B. Wood. 1996. Transformations of 2:1 phyllosilicates in 41-year-old soils under oak and pine. Geoderma 70:49–62.
Torrent, J., W.D. Nettleton, and G. Borst. 1980a. Genesis of a Typic Durixeralf of southern California. Soil Sci. Soc. Am. J. 44:575–582.
Torrent, J., U. Schwertmann, and D.J. Schulze. 1980b. Iron oxide mineralogy of some soils of two river terrace sequences in Spain. Geoderma 23:191–208.
Woodruff, G.A. 1978. Soil survey of San Bernardino County, southwestern part, California. U.S. Gov. Print. Office, Washington, DC.